

Comparison of different types of self-healing concrete under extreme conditions

Vanessa G. Cappellesso^{1,2}, Tim Van Mullem¹, Elke Gruyaert², Kim Van Tittelboom¹ and Nele De Belie^{1*}

¹Ghent University, Department of Structural Engineering and Building Materials, Technologiepark Zwijnaarde 60, 9052 Ghent, Belgium

²KU Leuven, Department of Civil Engineering, Materials and Constructions, Ghent Technology Campus, Gebroeders De Smetstraat 1, 9000 Ghent, Belgium

Abstract. Extreme environments are aggressive for concrete structures, hence a performance-based design is crucial to guarantee the durability during the service life. Nonetheless, there is a knowledge gap regarding the influence of cracks on standard and self-healing concrete. This research focuses on monitoring cracked self-healing concrete with two commercial healing agents: a bacteria-based healing agent (BAS) and a crystalline admixture (CA). After crack formation and a healing process of three months in wet/dry conditions (4 days/3 days), several extreme conditions were considered: (1) submerged in artificial seawater, (2) submerged in a solution with 33 g/L sodium chloride and (3) freeze-thaw (FT) cycling with de-icing salts. Microscopic images were used to quantify the healing efficiency of the two different healing agents, while chloride ingress and scaling were measured to determine durability. The results of the microscopic measurements indicated significant healing efficiency for both healing agents after the healing regime reaching 72% for CA, and 67% for BAS. After exposure to a marine environment, this efficiency increased to 95% and 92%, respectively. The uncracked BAS samples achieved a scaling reduction of 93% under FT exposure relative to the uncracked REF samples, while this was 49% for the CA samples. In cracked samples, scaling was reduced by 50% for BAS and 24% for CA, relative to the cracked REF samples. In all tested conditions, the BAS samples partially prevented the chloride ingress through the crack, while CA samples showed a great reduction. Overall, both healing agents reduced the degradation and could decrease the chloride ingress.

1 Introduction

Self-healing concrete plays an essential role in maintaining the durability of concrete structures. Recently, a considerable amount of papers have been published focusing on the application of healing agents to boost the self-healing ability of concrete. The aim is to introduce some materials in the concrete mix with the potential to close cracks and block the aggressiveness from the environment, which further degrades the concrete structure if the pathway is kept open. Several studies have been published showing significant improvements in crack closure with different self-healing technologies [1,2]. However, most of these studies focus only on evaluating crack closure in ideal conditions without exposure to environmental conditions. The ideal condition means giving the self-healing concrete the required trigger mechanism to guarantee crack closure. Generally, this is reached by bringing the crack in contact with water or with the essential trigger mechanism tailored for each healing agent. Nevertheless, there is uncertainty about how this self-healing concrete that reaches crack closure in ideal conditions can act as a barrier for aggressive substances in extreme environments.

Despite the exhaustive research focusing on self-healing concrete, only a few studies have investigated this technology in realistic conditions [3–5]. The outcomes of laboratory experiments may be ineffective when transferred to real environmental exposure. An extensive recent review paper has presented the need for studies focusing on self-healing concrete applications in natural conditions [6]. The paper critically reviews the lack of studies on self-healing concrete in realistic situations and how this evidence is fundamental for transferring the technology to the market. The main challenge faced by many researchers is how to mimic the realistic environment and test cracked concrete, while the standards prescribe methodologies only for non-cracked concrete. Furthermore, there is no proof of how each healing agent performs in different environmental conditions. Some healing agents may be good for certain situations but unsuitable for others. This calls for finding a tailored healing agent for each exposure condition considered.

This paper presents the results of an extensive experimental program to investigate two self-healing agents in three mimicked realistic conditions. The healing took place while being exposed to ideal conditions, while the healed samples were exposed

* Corresponding author: nele.debelie@ugent.be

afterwards to extreme conditions. The two healing agents are a bacteria-based healing agent and a crystalline admixture. Concrete specimens with those healing agents were subjected to three different environmental conditions after the healing regime: (1) submerged in artificial seawater, mimicking a marine environment, (2) submerged in a solution with 33 g/L sodium chloride, mimicking a chloride-rich environment and, (3) freeze-thaw (FT) cycling with de-icing salts, mimicking a cold climate that suffers from cyclic freezing and thawing and the presence of de-icing salts. The specimens had a crack of around 300 µm in width. They were healed for three months in a cyclic wet/dry regime of four days submerged in demineralised water and three days drying to allow healing of the cracks, before being subjected to extreme conditions. The healing regime was performed to evaluate the efficiency of the healing product in blocking the ingress of aggressive solutions through the crack. The self-healing concrete was compared to a reference concrete without any healing agent. This study provides new insights into the behaviour of self-healing concrete exposed to extreme conditions after crack healing.

2 Materials and methods

2.1 Concrete compositions

Three mix designs were considered: a reference (REF) concrete without any healing agent, concrete containing bacteria as a healing agent (BAS), and a concrete with crystalline admixture in the composition (CA). The concrete compositions are given in Table 1.

Table 1. Concrete mix compositions, in kg/m³.

Concrete composition	REF	BAS	CA
CEM I 52.5 N	340.0	337.1	339.7
Sand 0/4 mm	748.3	741.8	747.6
Gravel 2/8 mm	1038.5	1029.5	1037.6
Limestone filler	58.4	57.9	58.4
Crystalline admixture	-	-	2.7
Bacteria-based agent	-	10.1	-
Water	170.0	168.5	169.9
Superplasticizer (BASF) MasterGlenium 27	2.0	2.0	2.0

Table 2 shows the results obtained for the control tests performed in the fresh state: density [7], air content [8] and flow table [9]. The compressive strength was tested on three cubes of 150 mm side length [10]. Two cubes of 100 mm side length were cast for air void analysis, an automated test to analyse the spacing factor of hardened concrete as described in ASTM C 457 [11].

Table 2. Fresh and hardened properties of the concrete.

Properties	REF	BAS	CA
Density (kg/m ³)	2388	2344	2350
Air content (%)	2.8	2.5	2.0
Flow (mm)	540	560	520

Compressive strength at 28 days (MPa)	57.22±1.23	60.38±1.01	59.18±1.27
Spacing factor at 28 days (µm)	303±83	381±79	350±94

2.2 Healing agents

Two commercial healing agents were applied in this study. Both products have water as a trigger mechanism to activate the healing phenomenon. The bacteria-based healing agent was supplied by Basilisk (the Netherlands). The healing agent is available in powder form with a particle size of 0.5-2 mm. It is composed of polylactic acid (50-80 wt%), bacterial spores of *Bacillus cohnii* (0.1-2 wt%), nutrients being calcium lactate as a calcium source (10.5-43 wt%), and moisture (1-5 wt%) [12]. The suitable dosage for concrete varies between 5 to 15 kg/m³. In this research, the concrete mix design contains 10.1 kg/m³, representing 3% by the weight of the cement.

The other healing agent is a crystalline admixture provided by Penetron (Italy). The suggested dosage is between 0.8 and 1% of the cement weight. In this research, 0.8% of the cement weight was chosen. The composition of this healing agent has been kept a trade secret, although some information can be found in the literature [13].

2.3 Specimens preparation

Reinforced prisms with dimensions of 60 x 60 x 220 mm³ were cast to be tested in marine and chloride environments. The reinforcement consisted of two smooth cooper-coated steel wires of 2 mm in diameter placed in the bottom of the formwork at 10 mm from each side. For FT conditions, were cast cylinders of 50 in height and 100 mm in diameter. All specimens were kept in an air-conditioned room (at 20 ± 2°C and at least 95 % relative humidity) for 28 days. The samples were cracked at 28 days. On the prisms, cracks were created by three point-bending tests, while on cylinders, a Brazilian splitting test was used. In both cases, crack widths were controlled by a Linear Variable Differential Transformer (LVDT). The aim was to introduce a 300 µm wide crack.

The prisms were sawn after the crack creation, reducing the length from 220 mm to 80 mm, keeping the crack in the middle. The edges which were sawn off were used as uncracked specimens. The sides of the samples were coated by an epoxy resin to guarantee contact with the aggressive environment only the surface where the crack was located was kept uncoated, i.e., five out of six sides were coated.

2.4 Healing regime

The specimens were healed after the crack creation. The healing regime lasted for three months to boost the self-healing ability of the self-healing concrete. Both cracked and uncracked samples were kept in the same condition.

The healing condition consisted of weekly wet-dry cycles where the samples were kept for four days submerged in demineralised water and three days drying in laboratory conditions.

2.5 Exposure conditions

The specimens were pre-saturated by submersion in demineralised water for two days before being brought into contact with the salt solutions. In all conditions, demineralised water was used to make the solutions. For the marine and chloride environment, a ratio of 80 between the exposed concrete surface area (cm²) and the volume of the solution (dm³) was considered. The containers with solution were kept in an air-conditioned room (20°C and 60% relative humidity).

2.5.1 Marine environment (Mar)

The marine environment was performed for three months under a mimicked condition by preparing an artificial seawater solution. The composition of the solution is prescribed in ASTM D1141-98 [14]. The standard prescribes the composition of substitute ocean water with heavy metals. In this research, heavy metals were not included in the exposure solution. The composition used is described in Table 3.

Table 3. Artificial seawater (ASTM D1141-98, 2021).

Compound	Concentration (g/L)
NaCl	24.53
MgCl ₂	5.2
Na ₂ SO ₄	4.09
CaCl ₂	1.16
KCl	0.695
NaHCO ₃	0.201
KBr	0.101
H ₃ BO ₃	0.027
SrCl ₂	0.025
NaF	0.003

2.5.2 Chloride environment (Cl)

The chloride environment was realised by submerging the specimens in a solution with 33 g/L of NaCl. The experiment had a duration of three months.

2.5.3 Freeze-thaw (FT) with de-icing salts

The FT exposure was based on the standard (EN 12390-9, 2016) [15]. The entire procedure is described in Cappellesso et al.[16]. It consists of cycles where the temperature changes from -20°C to 20°C in 24 hours, each day representing one cycle, and the test runs up to 56 cycles. The specimens were covered by a 3 mm layer of 3% NaCl salt solution.

2.6 Test methods

2.6.1 Crack measurements

The crack widths were defined by taking at least 20 measurements along the crack length at the top side of the specimens. The measurements were executed with a stereomicroscope, Leica S8 APO, with DFC 295 camera. The same spots were analysed before and after the healing regime to define the self-healing efficiency (SE) in percentage by using equation 1. Where CW represents the average crack width per specimen (i) at the time zero (t₀) being right after crack creation, and after the healing regime (t_{healed}).

$$SE_i [\%] = \frac{CW_i^{t_0} - CW_i^{t_{healed}}}{CW_i^{t_0}} \times 100\% \quad (1)$$

The same equation (1) can be used to define SE after exposure to the mimicked extreme conditions. In the case of marine and chloride environments, the analysis was performed after one and three months of exposure. Note that the crack width measurements after FT conditions could not be taken after exposure due to the degradation of the exposure surface.

2.6.2 Scaling measurements

During FT exposure, the scaled material was collected at time steps as specified in the standard EN 12390-9 [15]. To collect the scaled material from the test surface, the surface was rinsed with demineralised water using a spray bottle. A scaling reduction coefficient (SR) was calculated using the accumulated scaled material obtained at 56 days to verify the potential reduction. The SR was obtained by subtracting the accumulated scaled material of the healing agent series (SR_{HA}) from the accumulated scaled material of the reference series (SR_{REF}) and dividing it by SR_{REF}.

$$SR [\%] = \frac{SR_{REF} - SR_{HA}}{SR_{REF}} \times 100\% \quad (2)$$

The result shows how much the concrete with the healing agent improved the resistance by reducing the scaling, hence, the concrete degradation. The coefficient was calculated both for the uncracked and cracked series.

2.6.3 Chloride ingress

A silver nitrate solution with 0.1 mol/L was sprayed on the sample halves to visualise the chloride ingress by colour change boundary in all exposure conditions. Extra attention was given to the cracked specimens, which had the silver nitrate sprayed onto faces perpendicular to the crack. A similar procedure was used in previous research [16].

3 Results and discussions

3.1 Crack widths and crack closure

The crack width at crack creation (CR) was aimed to reach around 300 μm . After the healing regime (AH), the cracks were verified again in order to calculate the SE. For Mar and Cl conditions, two measurements were made during and after exposure, the first at one month (1) and the last at three months (3) of exposure. The crack widths obtained for the FT series are given in Fig. 1 and the error bars represent the standard deviation.

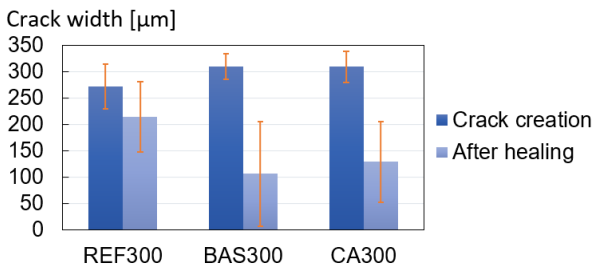


Fig. 1. Crack width measurements over time in FT specimens.

The specimens of the FT series could reach the aimed crack width. The REF series showed a SE of 21%, while the BAS series had a better self-healing performance with a SE of 66%. CA also showed a great healing ability with an SE of 58%.

Fig. 2 shows the measurements for the series exposed to a marine environment. The CA series obtained a narrow crack width compared to the REF and BAS series. Note that the FT series consisted of cylindrical samples, while the samples exposed to a marine environment were prismatic. For the CA series showed 72% of SE, while for the REF series only 16% crack sealing was noticed. On the other hand, BAS, even with the larger crack width, reached a considerable SE of 67%. After exposure, for the REF concrete the SE increased to 72% after one month, reaching a value of 74% after three months when subjected to a marine environment. BAS had a SE of 85% after one month and 92% after three. CA had a better performance reaching 92% after one month and 95% after three months.

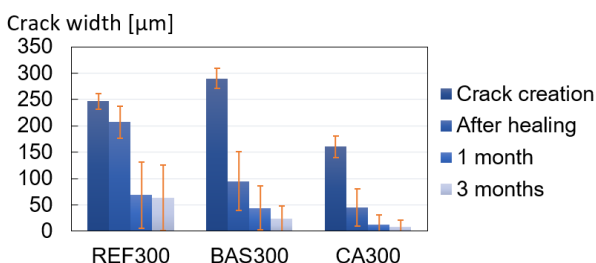


Fig. 2. Crack width measurements over time in specimens subjected to marine environment.

For the Cl series, the results are presented in Fig. 3. The BAS series obtained a narrower crack width compared to the REF and CA in this case. Consequently, BAS also showed a higher crack closure that could be partly related to the initial crack width and the interaction with the chloride environment. The BAS series had the highest SE of 50% after the healing regime reaching 100% after three months in a chloride solution. In this

condition, REF and CA had similar behaviour after the healing regime and also after the exposure. Both REF and CA reached almost 100% SE after exposure.

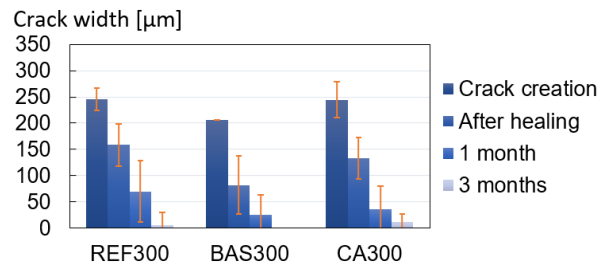


Fig. 3. Crack width measurements over time in specimens subjected to chloride environment.

In Fig. 4 an overview is given of the SE obtained in the different exposure conditions. In general, the healing agents improved the performance compared to REF concrete. BAS and CA had SE values close to 60% for the FT and Mar conditions, while for REF this was around 20%. Only for the Cl conditions, the difference was small between the self-healing concrete and the REF series. When the SE is considered after exposure, Cl conditions had a higher impact on the crack closure, reaching almost 100% for both healing agents. On the other hand, for the Mar condition, BAS concrete and CA reached a SE of around 95%, while REF showed around 70% of SE.

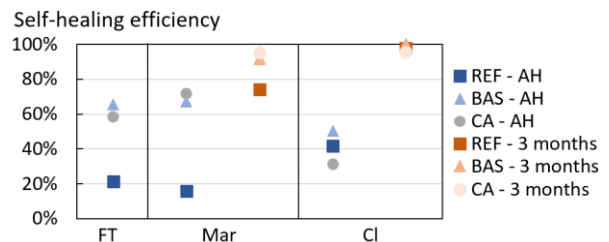


Fig. 4. Self-healing efficiency after healing regime (AH) and after three months in the respective environmental conditions: marine environment (Mar) and chloride environment (Cl).

3.2 Scaling measurements

The outcomes for the scaling measurements for both cracked and uncracked series are given in Fig. 5. The results show the accumulated scaled material per surface area during the 56 cycles. REF series showed a higher degradation by the FT cycles. The CA series proved a beneficial reduction in scaling. The BAS series performed best. These results are in agreement with previous analyses [16]. For all series, the uncracked samples had less scaling when compared to cracked samples. The worse performance of the cracked samples confirms that when damage is present, in this case a crack, the degradation is accelerated. It supports the need to use self-healing concrete to close the crack before the damage advances to the worst situation.

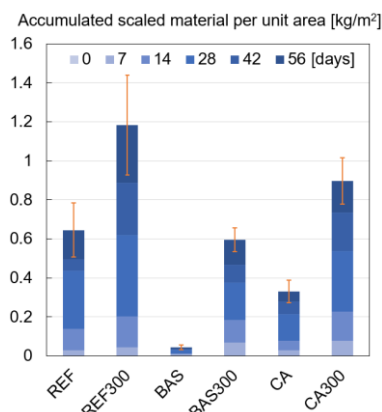


Fig. 5. Scaling results for the series subjected to FT.

When the scaling reduction coefficient is observed (Fig. 6), it is possible to verify the benefit of using the healing agents. BAS had a SR of 93% in the uncracked samples, while even with the presence of a crack, the SR reached almost 50% when compared to REF cracked samples. The CA series also achieved an important reduction in the degradation by FT, with the CA uncracked series showing similar scaling to the BAS cracked series. In both cases, the presence of the crack increased the scaled material and there was almost 50% reduction of the SR compared to the SR of their respective uncracked samples.

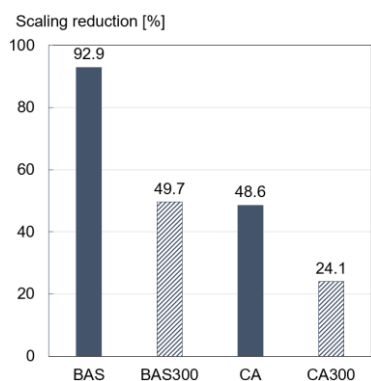


Fig. 6. Scaling reduction coefficient (SR) of the series containing healing agents compared to their respective reference samples (uncracked or cracked).

3.3 Chloride ingress

The ingress of chlorides plays a crucial role related to durability. Fig. 7 shows the results of chloride ingress for the uncracked series after exposure. The variability in the results was higher in the marine environment, probably due to the combined salt attack being a complex mechanism which changes with exposure time. The healing agents helped in reducing chloride ingress in FT and Mar situations. The BAS series performed superior in the FT condition, presumably due to the densification of the matrix caused by the use of the bacteria-based healing agent. These findings agree with the scaling results. A similar result was found in the Mar condition. However, for the Cl condition, BAS showed slightly higher Cl ingress than REF. In the case of the CA series, the behaviour in Mar and Cl conditions was close to BAS, but chloride ingress was higher than for BAS when considering the FT condition.

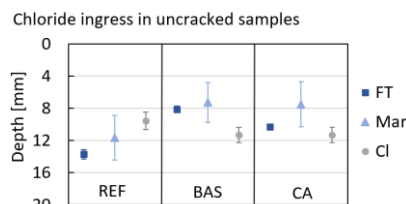


Fig. 7. Chloride ingress in uncracked samples.

The results in Fig. 8 demonstrate the chloride ingress in cracked samples after FT, where the chloride ingress was similar for all series. The evidence indicates that the cyclic freeze-thaw destroyed the healing products in the crack. On the other hand, the healing agents induced a consistent improvement in the concrete mix that could reduce the scaling as discussed in section 3.2.

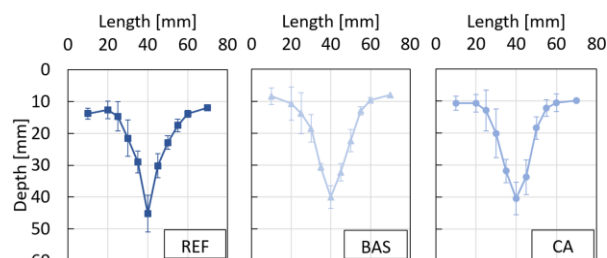


Fig. 8. Chloride ingress in cracked samples subjected to FT

In the Mar condition (Fig. 9), the chloride ingress was greatly reduced for the CA series. The same evidence for the CA series can be seen in the Cl condition (Fig. 10). It demonstrates that the CA used as a healing agent could partly prevent the chloride ingress, decreasing around 40% compared to the REF series in both conditions. The BAS series showed an unexpected behaviour in the Mar condition (Fig. 9), where chloride ingress was unexpectedly higher.

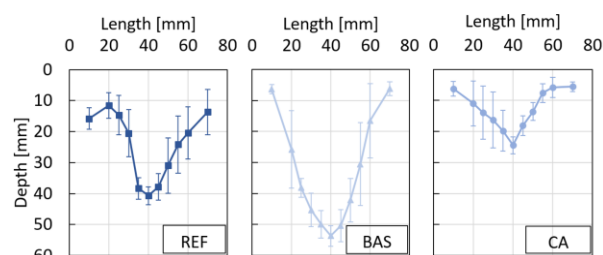


Fig. 9. Chloride ingress in cracked samples subjected to Mar.

Note that the crack width was larger for the BAS series which might have contributed to reducing the internal self-healing efficiency. Another reason could be the higher crack depth obtained in the BAS series as this test was carried out on prisms which were cracked via a 3-point bending test. Another point could be related to the fact that the bacteria-based healing agent produces calcium carbonate (CaCO_3) as a healing product, and an excessive presence of CO_3^{2-} could cause a false positive result with the silver nitrate indicator [17]. The silver ions (Ag^+) can react with CO_3^{2-} producing Ag_2CO_3 (silver carbonate), which also results in a whitish colour.

In contrast, an opposite behaviour was identified in the Cl condition (Fig. 10). This might suggest that beyond the bacterial activity in CaCO_3 production, the salts in the mimicked seawater could also affect the performance obtained by the BAS series. Consequently, a more detailed investigation is needed for the BAS

series and should reveal what caused the different results obtained for the Mar and Cl conditions. Overall, the chloride ingress in the Cl condition was reduced for both healing agents.

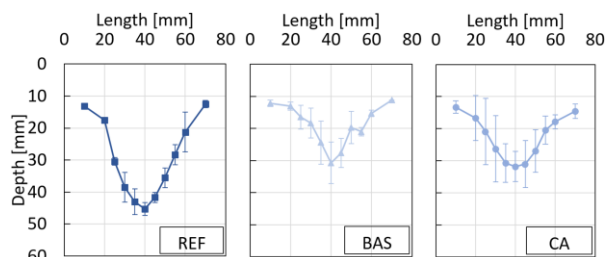


Fig. 10. Chloride ingress in cracked samples subjected to Cl.

4 Conclusions

The presented results help to understand the behaviour of two different types of self-healing concrete (with either crystalline admixture or bacterial agent) in realistic extreme conditions. Both healing agents showed excellent performance improving the behaviour compared to the uncracked samples by at least 50% for CA and 93% for BAS, considering the freeze-thaw with de-icing salts representing a cold climate. When cracked samples were considered, they showed a scaling reduction of at least 24% for CA, and could reach 50% for BAS. However, the healing agents could not prevent the chloride ingress through the crack.

In the marine environment, the CA showed the best performance, blocking the ingress of chloride and preventing it from penetrating more than 25 mm in depth, while for REF, the ingress almost reached 40 mm. The BAS series must be further investigated in this condition to understand why it had a rather negative effect on Cl ingress. In the case of the chloride environment, the CA and BAS showed similar improved behaviour related to chloride ingress, while REF had an ingress of about 1.5 times more than the self-healing concrete. Considering the results of the cracked specimens, CA had a better behaviour in preventing the chloride ingress than BAS, while BAS was more effective in reducing FT damage. However, both healing agents improved the concrete mix by increasing durability.

This study provided a significant opportunity to advance the understanding of self-healing concrete in realistic environments. It further indicates how the healing agents could perform in those realistic conditions. The findings showed the benefits caused by using healing agents in concrete compositions and how they can improve durability by reducing degradation and chloride ingress, although more research is needed to improve the healing efficiency further.



This project has received funding from the European Union's Horizon 2020 research and innovation programme under the Marie Skłodowska-Curie grant agreement No 860006.

References

1. N. De Belie, E. Gruyaert, A. Al-Tabbaa, P. Antonaci, C. Baera, D. Bajare, A. Darquennes, R. Davies, L. Ferrara, T. Jefferson, C. Litina, B. Miljevic, A. Otlewska, J. Ranogajec, M. Roig-Flores, K. Paine, P. Lukowski, P. Serna, J.-M.M. Tulliani, S. Vucetic, J. Wang, H.M. Jonkers, *Adv. Mater. Interfaces.* 5 , 1–28 (2018).
2. L. Ferrara, T. Van Mullem, M.C. Alonso, P. Antonaci, R.P. Borg, E. Cuenca, A. Jefferson, P.-L. Ng, A. Peled, M. Roig-Flores, M. Sanchez, C. Schroefl, P. Serna, D. Snoeck, J.M. Tulliani, N. De Belie, *Constr. Build. Mater.* 167, 115–142 (2018).
3. V.G. Cappelleso, T. Van Mullem, E. Gruyaert, K. Van Tittelboom, N. De Belie, *Self-healing bacterial concrete exposed to freezing and thawing associated with chlorides*, in: *Proc. Resilient Mater. 4 Life 2020*, Cardiff University, Cardiff, UK, 241–246 (2021).
4. E. Cuenca, S. Rigamonti, E. Gastaldo Brac, L. Ferrara, , *J. Mater. Civ. Eng.* 33, 04020491 (2021).
5. E. Rossi, R. Roy, O. Copuroglu, H.M. Jonkers, *Constr. Build. Mater.* 319, 126081 (2022).
6. V. Cappelleso, D. di Summa, P. Pourhaji, N. Prabhu Kannikachalam, K. Dabral, L. Ferrara, M. Cruz Alonso, E. Camacho, E. Gruyaert, N. De Belie, *Int. Mater. Rev.* 1–48 (2023).
7. EN 12350-6 (2019).
8. EN 12350-7 (2019).
9. EN 12350-5 (2019).
10. NBN EN 12390-3 (2019).
11. ASTM C457 (2016).
12. R. Mors, H.M. Jonkers, *Bacteria-based self-healing concrete: evaluation of full scale demonstrator projects*, *RILEM Tech. Lett.* 4, 138–144 (2020).
13. M. Nasim, U.K. Dewangan, S. V. Deo, *Mater. Today Proc.* 32, 638–644 (2020).
14. ASTM D1141 – 98 (2021).
15. NBN EN 12390-9 (2016).
16. V.G. Cappelleso, T. Van Mullem, E. Gruyaert, K. Van Tittelboom, N. De Belie, *Bacteria-based self-healing concrete exposed to frost salt scaling*, Under Submiss. (2023).
17. C.V. Pontes, G.C. Réus, E.C. Araújo, M.H.F. Medeiros, *J. Build. Eng.* 34 101860 (2021).